scientific reports

OPEN

Nanoscale thermal control of a single living cell enabled by diamond heater-thermometer

Alexey M. Romshin[1✉], Vadim Zeeb[2✉], Evgenii Glushkov[3], Aleksandra Radenovic[3], Andrey G. Sinogeikin[4] & Igor I. Vlasov[1]

We report a new approach to controllable thermal stimulation of a single living cell and its compartments. The technique is based on the use of a single polycrystalline diamond particle containing silicon-vacancy (SiV) color centers. Due to the presence of amorphous carbon at its intercrystalline boundaries, such a particle is an efficient light absorber and becomes a local heat source when illuminated by a laser. Furthermore, the temperature of such a local heater is tracked by the spectral shift of the zero-phonon line of SiV centers. Thus, the diamond particle acts simultaneously as a heater and a thermometer. In the current work, we demonstrate the ability of such a Diamond Heater-Thermometer (DHT) to locally alter the temperature, one of the numerous parameters that play a decisive role for the living organisms at the nanoscale. In particular, we show that the local heating of 11–12 °C relative to the ambient temperature (22 °C) next to individual HeLa cells and neurons, isolated from the mouse hippocampus, leads to a change in the intracellular distribution of the concentration of free calcium ions. For individual HeLa cells, a long-term (about 30 s) increase in the integral intensity of Fluo-4 NW fluorescence by about three times is observed, which characterizes an increase in the $[Ca^{2+}]_{cyt}$ concentration of free calcium in the cytoplasm. Heating near mouse hippocampal neurons also caused a calcium surge—an increase in the intensity of Fluo-4 NW fluorescence by 30% and a duration of ~ 0.4 ms.

Despite the constantly growing interest in local thermodynamic phenomena at micro and nanoscale in living cells and organisms in the last three decades[1–17], living cell thermodynamics is still a matter of guesses and controversies[18–21].

Discoveries of the faster neurite growth aligned with a local thermal gradient[10], heat-pulse induced muscle contractions without Ca^{2+} influx[7] and highly thermosensitive Ca^{2+} dynamics in HeLa cells through IP3 receptors[6] put forward the idea that endogenous intracellular heat generation events could be useful for the concept of "thermal signaling"[16]. This suggests that a living cell relies on ultralocal temperature variations of endogenous origin for the regulation of multiple physiological processes.

As mentioned in Ref.[16], future progress in studying intracellular thermodynamics needs an instrumentation revolution allowing local control of thermogenesis at micro/nanoscale, control of heat dissipation and heat energy conversion to other electrochemical energy types.

Currently, the development of new instruments for exploring intracellular thermodynamics mostly follows the idea of constructing Heater/Thermometer (HT) nanohybrids, combining nanomaterials able to generate heat and detect temperature. Multiple systems, such as metallic nanoparticles[22] and polymer coatings[23], efficiently transforming laser illumination into heat, have been reported as promising nanoscale heaters. Other materials, such as rare-earth complexes[24], quantum dots[25] and diamond nanocrystals with nitrogen-vacancy (NV)[12,15,23] and silicon-vacancy (SiV) centers[26], have been used to measure local temperature changes through the temperature-induced shift of their luminescence. However, such a hybrid HT approach complicates its practical use as one has to reproducibly match two nanostructures with different properties to form a hybrid one. Main disadvantages of the existing hybrid HTs include (= 1)—the need to use a large number of hybrid nanoparticles in one experiment,

[1]Prokhorov General Physics Institute of the Russian Academy of Sciences, Vavilov str. 38, Moscow 119991, Russia. [2]Institute of Theoretical and Experimental Biophysics of the Russian Academy of Sciences, Pushchino, Moscow Region 142292, Russia. [3]Laboratory of Nanoscale Biology, Institute of Bioengineering, Ecole Polytechnique Federale de Lausanne (EPFL), 1015 Lausanne, Switzerland. [4]NanThermix SA, Ecole Polytechnique Federale de Lausanne (EPFL) Innovation Park, 1015 Lausanne, Switzerland. ✉email: alex_31r@mail.ru; zeebvad@gmail.com

(= 2)—uncontrolled variations in heating properties from particle to particle, (= 3)—the impossibility of preliminary calibration of an individual HT in terms of heating and temperature sensing, (= 4)—the sensitivity to parameters of the external environment, in particular, pH.

We propose a design of a nanoscale heater/thermometer that is free from the disadvantages listed above. The device is based on the combination of the properties of a heater and a thermometer in a single material—a polycrystalline diamond nanoparticle, and the use of only one HT, pre-calibrated in terms of temperature and heating, intended for experiments on ultralocal thermal effects in single cells and subcellular structures. Contrary to the above-mentioned hybrid HTs, such individually pre-calibrated DHT can be reliably used for precise thermal control at the nanoscale.

To demonstrate the capabilities of the developed diamond heater-thermometer (DHT), we present the results on thermal induction of intracellular calcium events in single cells (HeLa and neurons), where calcium is used as an established intra/extracellular signaling agent[27].

Experimental details

DHT design and operation.
The design principle of the DHT device follows that of the diamond thermometer described in detail in Ref.[1]. It consists of a polycrystalline CVD diamond particle embedded at the end facet of a submicron-diameter glass capillary (Fig. 1, inset). The operating principle of the device is based on the dependence of the position of the maximum of the zero-phonon line (ZPL) luminescence of the "silicon-vacancy" (SiV) centers in the diamond particle (Fig. 2a) on temperature[1], as well as on the ability of a diamond particle to absorb laser radiation due to the presence of amorphous carbon at its intercrystalline boundaries.

Before experimental use, a double calibration of the diamond particle is performed: via controlled temperature and via laser heating. The first calibration curve represents the dependence of the spectral position of the maximum of the zero-phonon luminescence line of SiV centers on a given temperature (Fig. 3a, see "Methods"). To perform the second calibration, a diamond particle fixed in a glass capillary is placed in the medium under study and the dependence of the heating temperature of the diamond nanoparticle on the power of the laser radiation focused on the particle is determined (Fig. 3b, see "Results"). The temperature calibration of a DHT was carried out in the low-power illumination regime ($P_{laser} < 0.5$ mW), when the laser-induced heating of the
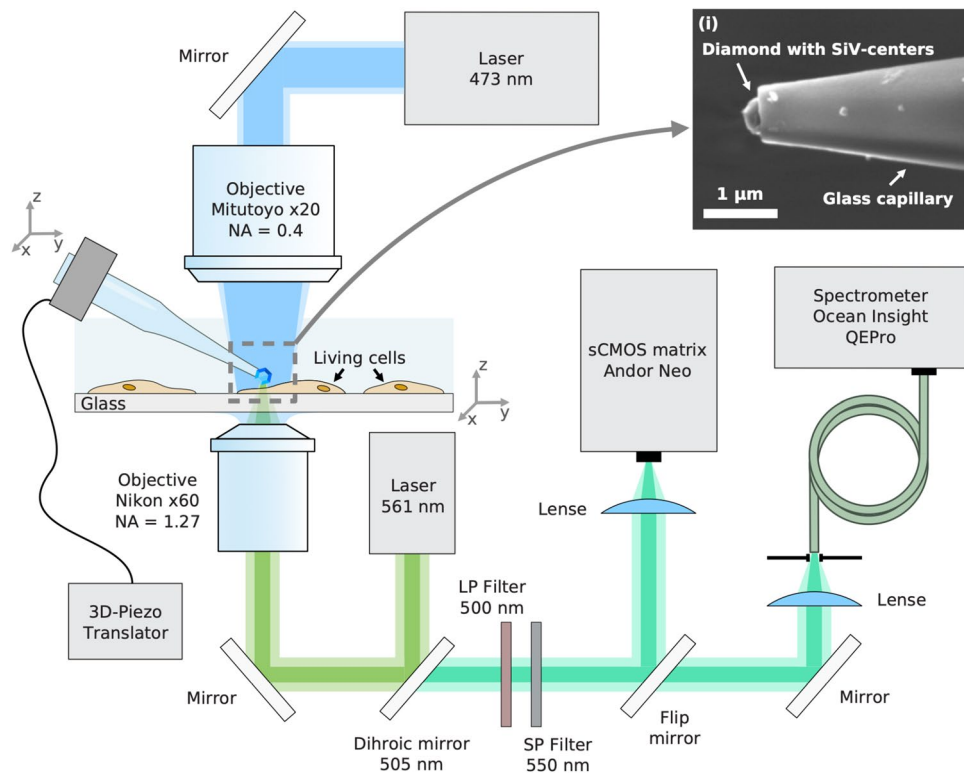

Figure 1. Schematic of the experimental setup for measuring the fluorescent response of the Fluo-4 NW dye in cells, and for tracking the luminescence of SiV centers in diamond. Two independent moving platforms are used: the coverslip seeded with living cells is fixed at the 3D-piezo stage, while the DHT is attached to the three-axis micromanipulator. The 473 nm laser beam illuminates the top side of the living cells through the low-NA objective. The excited Fluo-4 NW fluorescence collected from the bottom of the coverslip through the water-immersion objective (Nikon 60x, WI, NA = 1.27) is then either projected on an sCMOS camera or sent to the spectrometer, depending on the position of the flip mirror. The 561 nm laser was used to excite the SiV-luminescence and to induce the heating; the inset (i) shows the SEM image of a submicron glass capillary with the diamond nanoparticle localized at the tip.
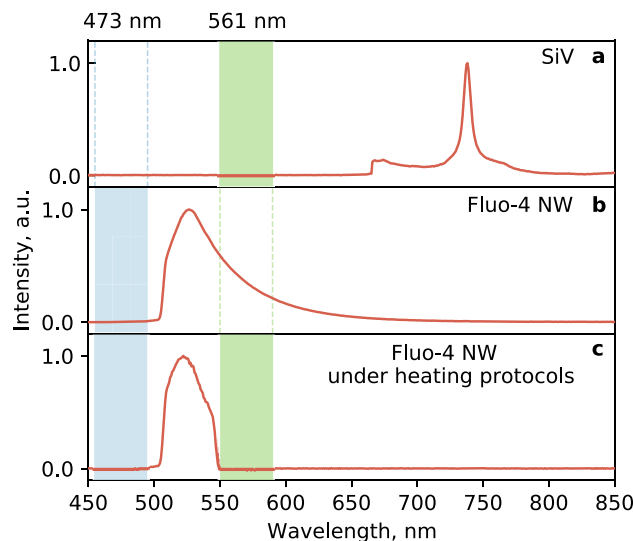
Figure 2. Characteristic experimentally-recorded emission spectra of: (**a**) the SiV-luminescence with 561-excitation, (**b**) Fluo-4 NW without the DHT with 473-excitation and (**c**) Fluo-4 NW following the DHT-heating protocol utilizing both 473 and 561 nm excitation lines simultaneously. The fluorescence signal is filtered out using a combination of short pass and long pass filters in the 505–550 nm range.
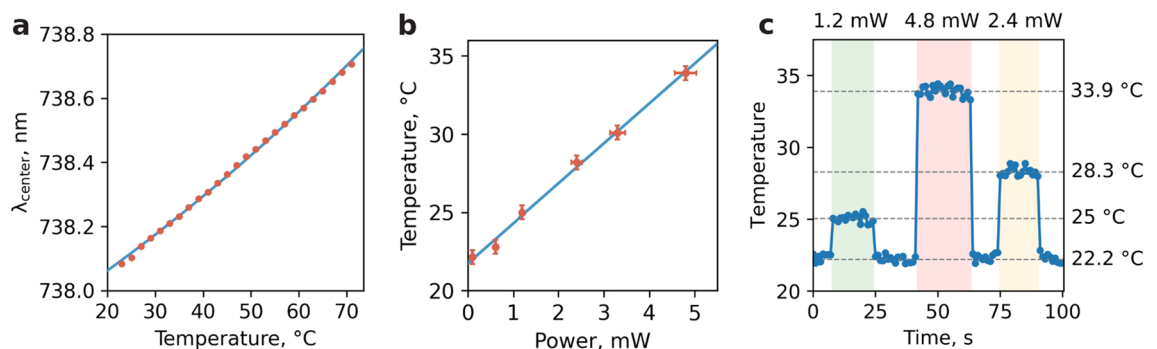

Figure 3. (**a**) The calibration dependence of the ZPL spectral position from the temperature in the thermostat. The thermal sensitivity of the DHT's spectral shift was determined to be ~ 0.01 nm/°C; (**b**) The heating temperature calibration dependence on illumination power at 561 nm; (**c**) Temporal changes in the heating temperature of a diamond particle at three different values of the illumination laser power (upper part of the graph). At a temperature of 22.2 °C, the measured laser power before the objective was 0.2 mW; therefore, the baseline of the dependence (lower dashed line) characterizes the unperturbed system. An increase in illumination power leads to a proportional increase in temperature, which reaches its maximum $T_{max} = 33.9$ °C at 4.8 mW.

particle is negligible (< 0.1 °C). In contrast, the heating calibration was carried out by sweeping the laser power 1–5 mW range.

Therefore, a DHT is capable of operating in two modes. At higher laser power, it operates as the local heater and thermometer simultaneously. At low laser excitation (< 0.5 mW) this device does not produce heating and operates as a thermometer.

Experimental setup. The study of the effect of local heating on living cells was carried out using a home-built confocal luminescent spectrometer (Fig. 1). Two lasers were used in the experiment: one to heat up the diamond particle, and the second one to excite the luminescence of the Fluo-4 NW dye used to visualize $[Ca^{2+}]_{cyt}$ in cells. The diamond particle was heated by a PicoQuant laser source at a wavelength of 561 nm, which was directed to the input of a water immersion objective focusing it on the DHT from the bottom of the coverslip. The DHT itself was fixed on a highly sensitive 3D micromanipulator, to enable its precise positioning in the focal spot of the objective, producing local heat release near the object of interest.

The second laser line at a wavelength of 473 nm (LaserComb) was illuminating the coverslip surface from the top through a long working distance objective (Mitutoyo, 20×). This illumination excited the fluorescence of the dye in the cells that were in the field of view of the objective (~ 40 × 40 μm² area). The produced fluorescence near the surface of a selected living object was collected from the bottom of the coverslip through the

water-immersion objective (Nikon 60x, WI, NA = 1.27) and detected by a recording system consisting of an Andor Neo sCMOS camera and an Ocean Optics QEPro spectrometer. To filter out the spectral lines of laser sources, we used a combination of two optical filters LP 505 nm and SP 550 nm, effectively collecting the dye fluorescence from 505 to 550 nm (Fig. 2).

The fluorescence of Fluo-4 during the whole experiment was recorded at the same point where the diamond heater-thermometer was located. As a high numerical aperture objective was used, the volume of detection is determined by the optical resolution to be ~ 1 μm^3.

Results

The temperature dependence of the calcium dynamics in the cytoplasm of living cells $[Ca^{2+}]_{cyt}$ has been studied using the cultured HeLa cells and primary neurons, isolated from the mouse hippocampus. To visualize the $[Ca^{2+}]_{cyt}$ we used the commercially-available dye (Fluo-4 NW, Thermofisher), following the protocol from the manufacturer. Briefly, the cell medium in the well plate was replaced by a 1 ml of a buffer solution (1X HBSS, 20 mM HEPES) mixed with the Fluo-4 NW dye and probenecid.

The diamond heater was preliminarily calibrated using the recorded heating temperature dependence on the illumination power at 561 nm. To do this, we have replaced the filter set from Fig. 2c, by another one transmitting long-wave radiation above 700 nm from SiV centers (see Fig. 2a). The DHT was placed in a buffer solution away from living objects and the SiV luminescence spectra were measured and the temperature was subsequently determined with an integration time of 1 s and in steps of 1 s for 100 s (Fig. 3c). The resulting dependence shows three thermal steps with amplitudes of 25, 28.3, and 33.9 °C, depending on the 561 nm laser power (see Supplementary Information). Besides, the minimum detectable variation of temperature observed in experiment is ~ 0.12 °C at 10 s acquisition time (see Supplementary Information) and ~ 0.5 °C at 1 s acquisition time as shown in Fig. 3c which is naturally limited by the optics in use and errors in fitting the emission peak. In order to overlap time scales of the DHT and physiological response of the calcium fluorescent dye, the ~ 0.5 °C accuracy is chosen. This in turn determines the minimum controllable heating step at the level ~ 0.5 °C. Finally, the temperature 33.9 °C was chosen for working with the cells. We used 22 °C bath temperature given the fact that intracellular calcium dynamics is well presented in the whole range of temperatures from 22 to 37 °C as shown in Ref.[6].

At the next stage, the previously calibrated DHT was positioned next to a desired HeLa cell and fixed at a distance of ~ 0.2 μm from its surface. Then, at random moments, the 561 nm laser with a power of 4.8 mW was turned on for a short time (2–10 s) heating the diamond to 33.9 °C. Modeling the spatial temperature distribution of a spherical heat source in water[1] gives the maximum temperature close to the cell surface ≈ 29 °C. This temperature can be considered as instantly stabilized during the pulsed laser exposure (2–10 s), since the relaxation time to local thermal equilibrium in micron-scale aqueous medium is in the sub-millisecond range[4,28], resulting in stepwise temperature clamp close to the cell surface. A steep temperature gradient near the nanoscale heat source in the water[1] results in ~ 1 μm^2 effective heated area of the living cell under our experimental conditions.

Figure 4 demonstrated the temporal response of the integrated fluorescence intensity of the dye F/F_0, where F/F_0 is determined as $(F_{high} - F_{low})/F_{low}$. Here, F_{high} is the average of fluorescence intensities for 1 s after it reaches the maximum during Ca^{2+} overshoot, and F_{low} is the average of consecutive three to five data points immediately after heat pulse, obtained for several HeLa cells during heat stimulation. The distribution of free intracellular calcium changes abruptly after the end of the heat stimulation (marked in pink). Following the cooling phase, one of the cells (Fig. 4a) exhibits a prolonged (~ 30 s) increase in $[Ca^{2+}]_{cyt}$. ($3\times$ magnification F/F_0). After the completion of the temperature disturbance for 90 s and 140 s, short calcium bursts with a duration of less than one second and an amplitude (F/F_0) of $\sim 40\%$ were detected. On the tail of the dependence, starting from t = 150 s, the $[Ca^{2+}]_{cyt}$ level stabilizes, returning to the base level preceding the start of thermal stimulation. A similar increase in the intracellular level of free calcium immediately after the cooling phase is also observed for another cell (Fig. 4b). Here after 5 s of thermal exposure for 4 s, the fluorescence intensity (F/F_0) increases by 12%. Figure 4c shows a quasi-periodic temperature change (three protocols of stepwise heating of different duration), which allows
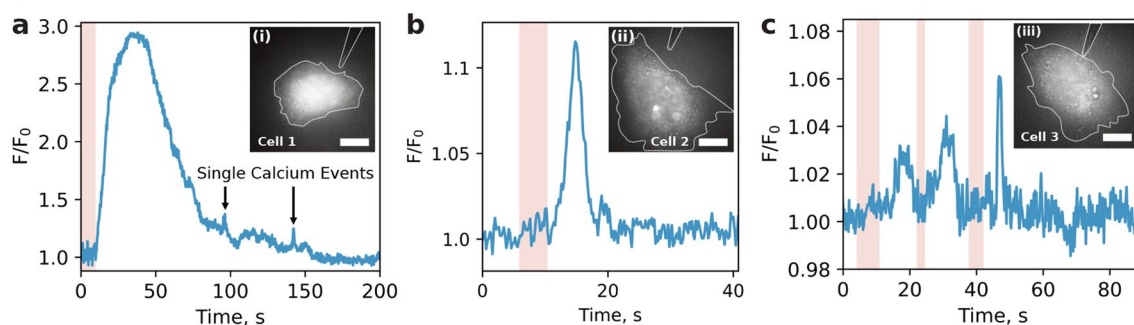

Figure 4. Time response of the normalized integrated fluorescence of Fluo-4 NW for three HeLa cells. The background component due to the presence of free calcium (plus the background noise of the recording system) in the buffer solution is experimentally measured beforehand and taken into account during normalization. The highlighted pink region indicates the time interval during which the heating was performed. The time resolution of each measurement is 0.2 s. Insets (i), (ii) and (iii) are the respective fluorescence images of HeLa cells before thermal stimulation. The dashed white lines prompt the outlines of cells and DHT. Scale bar: 10 μm.

one to effectively modulate in time the increase in the free concentration of calcium ions that occurs after each individual cooling phase of the temperature disturbance. Naturally, we were systematically performing control experiments on the possible effect of laser radiation in the absence of the DHT on the calcium response, as well as the response to the gentle touch of the probe itself in the absence of laser radiation. No changes in Fluo-4 fluorescence were observed in both control experiments.

We also performed a similar series of measurements with a primary culture of neurons isolated from the mouse hippocampus see Fig. 5. The neuron staining procedure was performed according to the protocol (Thermo Fisher Scientific, Inc., Waltham, MA, USA). In individual neurons, an extremely fast response to a step change in temperature was observed, which consisted in an increase in the normalized integral intensity of Fluo-4 NW $[Ca^{2+}]_{cyt}$ fluorescence by ~ 30% within 0.4 s. As in the case of HeLa cells, the general trend revealed was an increase in the intracellular concentration of free calcium ions after each individual cooling phase.

Discussion

In this work, we presented a new all-optical method for thermal stimulation of a single living cell with an accuracy of 0.1 °C[1] and a submicron spatial resolution, based on a DHT device. The main advantage of thermal stimulation with a DHT for a single living cell and its compartments is that the local temperature (temperature profile) is controlled reliably at a predefined point[1]. Moreover, the physical principles used to guarantee the absence of photobleaching in the DHT, enabling the use of unlimited experimental protocols for thermal stimulation of a living cell, which is impossible when using fluorescent temperature-sensitive sensors[3–5]. Combined with the biocompatibility of the DHT device, this creates a new method of stimulating a living cell and studying its enigmatic nanoscale heat transfer phenomena—the Nanoscale Temperature Control Method, providing a great flexibility of thermal stimulation and thermal control in comparison with the existing techniques.

As a particular example of the effectiveness of new ultralocal thermal stimulation, we demonstrated a change in the level of free intracellular calcium in individual HeLa cells and in the primary culture of neurons isolated from the mouse hippocampus. We have revealed the general effect of an increase in the level of intracellular concentration of free calcium after the end of the stepwise temperature perturbation of a single living cell. Whereas all types of thermally induced calcium responses appeared next to the stepwise temperature downfall phase, we monitor significant differences in time duration (time to peak) of thermally induced calcium elevations. These time durations range from fraction to tens of seconds suggesting superposition of multifarious calcium related intracellular processes[27]. This is similar to the effects reported in the literature, utilizing local stepwise heating of aluminum nanoparticles with a 1064 nm laser[6] as well as stepwise heating of water with a 1455 nm laser[29] utilizing a fluorescent EuTTA thermometer. These experiments describe the effects of local heating on calcium release from intracellular stores through IP3 receptors in Hela cells as well as calcium release through RYR1 Malignant Hyperthermia Syndrome mutants in human embryonic kidney 293 cells correspondingly. Thus, the heat induced calcium release was studied here at a higher level of confidence than has been done before[6,29] using the new method of ultralocal nano/microscale temperature control.

In this regard, the study of intracellular thermodynamics associated with various calcium events itself would require new methods. For instance, it has been shown that the functioning of calcium pumps (CaATPase) in the endo-sarcoplasmic reticulum of a living cell leads to significant thermogenesis[30] as the concentration gradient built by the pump increases. Cyclic calcium release in tuna fish muscle-derived heater organs (and in other big fishes) is the main suspect responsible for significant thermogenesis capable of keeping the eyes and brain of fish at 15 °C higher temperature in cold water[28]. Such data do not indirectly exclude the possible connection and synergy of universal intracellular calcium signaling with the thermal signaling concept[16].

Therefore, the fundamental importance of the new way of ultralocal temperature manipulation constitutes in the fact that it practically introduces this parameter into cellular physiology, namely into the privileged order of operational ultralocal parameters of the electrochemical potential equation[31,32] similarly to the transmembrane electric potential or ionic concentrations. This all-optical new tool is compatible with Patch Clamp[33] and Ca^{2+}
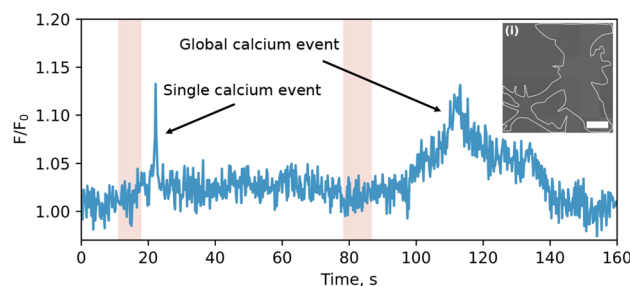
Figure 5. Time response of the normalized integrated fluorescence of Fluo-4 NW for a single neuron. The highlighted pink region indicates the time interval within which the heating was performed. The time resolution of each measurement is 0.2 s. The left calcium peak can be attributed to a rapid calcium spike, whereas the right one resembles a calcium wave since the cooling phase is followed by a steady calcium rise with time to peak at around half a minute. Inset (i) is the bright field image of the neuron before thermal stimulation. The dashed white lines prompt the outlines of cells. Scale bar: 10 μm.

imaging[34] and unambiguously tames the temperature at the nanoscale—the last parameter of the equation of electrochemical potential still escaping its precise ultralocal experimental control in intracellular compartments.

Methods

DHT calibration.   The developed DHT was placed in an air environment for a preliminary determination of the power density of optical excitation at a wavelength that did not lead to a shift of the zero-phonon SiV luminescence line, and, consequently, to heating. The measured power density was used to determine the temperature dependence of the spectral position of the zero-phonon line center in a Linkam TS1500 thermostat, stabilized at a predetermined level with an accuracy of ~ 1 °C. The temperature in the chamber was changed in increments of 10 °C. At each step, the SiV luminescence spectrum was recorded and the spectral position of the zero-phonon line maximum was determined according to the algorithm proposed in our previous work[1].

Cell culture.   Cell culture HeLa cells were cultured in Dulbecco's modified eagle's medium (DMEM) (Invitrogen, CA, USA) supplemented with fetal bovine serum (10%) and penicillin–streptomycin. The HeLa cell suspension was uniformly dispersed in a 2-in. Petri dish filled with 1 ml of the cell medium (DMEM) and cultured for 20 h. Cells were grown in a glass-based dish at 37 °C in the presence of 5% CO_2.

Primary neuron culture preparation.   Pregnant female C57BL/6J Rcc Hsd were obtained from Harlan Laboratories (France) and were housed according to the Swiss legislation and the European Community Council directive (86/609/EEC). Primary hippocampal cultures were prepared from mice brains from P0 pups as previously described[35]. The protocol was approved by the Swiss cantonal authorities VD, 'Service de la consommation et des affaires vétérinaires' Lausanne, Switzerland. Briefly, the hippocampi were isolated stereoscopically and dissociated by trituration in a medium containing papain (20 U ml^{-1}, Sigma-Aldrich, Switzerland). The neurons were plated on FluoroDish Sterile Culture Dish 35 mm, 23 mm well (World Precision Instruments), previously coated with poly-L-lysine 0.1% w/v in water, and neurons were cultured in Neurobasal medium containing B27 supplement (Life Technologies), L-glutamine and penicillin/streptomycin (100 U ml^{-1}, Life Technologies).

Data availability

All data generated or analyzed during this study are included in this published article.

References

1. Romshin, A. M. *et al.* A new approach to precise mapping of local temperature fields in submicrometer aqueous volumes. *Sci. Rep.* **11**, 14228 (2021).
2. Howarth, J. V. Heat production in non-myelinated nerves. *Philos. Trans. R. Soc. Lond. B Biol. Sci.* **270**, 425–432 (1975).
3. Chapman, C. F., Liu, Y., Sonek, G. J. & Tromberg, B. J. The use of exogenous fluorescent probes for temperature measurements in single living cells. *Photochem. Photobiol.* **62**, 416–425 (1995).
4. Zohar, O. *et al.* Thermal imaging of receptor-activated heat production in single cells. *Biophys. J.* **74**, 82–89 (1998).
5. Zeeb, V., Suzuki, M. & Ishiwata, S. A novel method of thermal activation and temperature measurement in the microscopic region around single living cells. *J. Neurosci. Methods* **139**, 69–77 (2004).
6. Tseeb, V., Suzuki, M., Oyama, K., Iwai, K. & Ishiwata, S. Highly thermosensitive Ca^{2+} dynamics in a HeLa cell through IP$_3$ receptors. *HFSP J.* **3**, 117–123 (2009).
7. Oyama, K. *et al.* Microscopic heat pulses induce contraction of cardiomyocytes without calcium transients. *Biochem. Biophys. Res. Commun.* **417**, 607–612 (2012).
8. Takei, Y. *et al.* A nanoparticle-based ratiometric and self-calibrated fluorescent thermometer for single living cells. *ACS Nano* **8**, 198–206 (2014).
9. Arai, S., Lee, S.-C., Zhai, D., Suzuki, M. & Chang, Y. T. A molecular fluorescent probe for targeted visualization of temperature at the endoplasmic reticulum. *Sci. Rep.* **4**, 6701 (2015).
10. Oyama, K. *et al.* Triggering of high-speed neurite outgrowth using an optical microheater. *Sci. Rep.* **5**, 16611 (2015).
11. Oyama, K. *et al.* Directional bleb formation in spherical cells under temperature gradient. *Biophys. J.* **109**, 355–364 (2015).
12. Kucsko, G. *et al.* Nanometre-scale thermometry in a living cell. *Nature* **500**, 54–58 (2013).
13. Zhou, J., Del Rosal, B., Jaque, D., Uchiyama, S. & Jin, D. Advances and challenges for fluorescence nanothermometry. *Nat. Methods* **17**, 967–980 (2020).
14. Choi, J. *et al.* Probing and manipulating embryogenesis via nanoscale thermometry and temperature control. *Proc. Natl. Acad. Sci.* **117**, 14636–14641 (2020).
15. Wu, Y. *et al.* Nanodiamond theranostic for light-controlled intracellular heating and nanoscale temperature sensing. *Nano Lett.* **21**, 3780–3788 (2021).
16. Okabe, K. & Uchiyama, S. Intracellular thermometry uncovers spontaneous thermogenesis and associated thermal signaling. *Commun. Biol.* **4**, 1–7 (2021).
17. Oyama, K., Ishii, S. & Suzuki, M. Opto-thermal technologies for microscopic analysis of cellular temperature-sensing systems. *Biophys. Rev.* **14**, 41–54 (2022).
18. Baffou, G., Rigneault, H., Marguet, D. & Jullien, L. A critique of methods for temperature imaging in single cells. *Nat. Methods* **11**, 899–901 (2014).
19. Kiyonaka, S. *et al.* Validating subcellular thermal changes revealed by fluorescent thermosensors. *Nat. Methods* **12**, 801–802 (2015).
20. Baffou, G., Rigneault, H., Marguet, D. & Jullien, L. Reply to: 'Validating subcellular thermal changes revealed by fluorescent thermosensors' and 'The 105 gap issue between calculation and measurement in single-cell thermometry'. *Nat. Methods* **12**, 803–803 (2015).
21. Suzuki, M., Zeeb, V., Arai, S., Oyama, K. & Ishiwata, S. The 105 gap issue between calculation and measurement in single-cell thermometry. *Nat. Methods* **12**, 802–803 (2015).
22. Taylor, M. L., Wilson, R. E., Amrhein, K. D. & Huang, X. Gold nanorod-assisted photothermal therapy and improvement strategies. *Bioengineering* **9**, 200 (2022).

23. Sotoma, S. *et al.* In situ measurements of intracellular thermal conductivity using heater-thermometer hybrid diamond nanosensors. *Sci. Adv.* **7**, eabd7888 (2021).
24. Bhaumik, M. L. Quenching and temperature dependence of fluorescence in rare-earth chelates. *J. Chem. Phys.* **40**, 3711–3715 (1964).
25. Maestro, L. M. *et al.* CdTe quantum dots as nanothermometers: Towards highly sensitive thermal imaging. *Small* **7**, 1774–1778 (2011).
26. Choi, S., Agafonov, V. N., Davydov, V. A. & Plakhotnik, T. Ultrasensitive all-optical thermometry using nanodiamonds with a high concentration of silicon-vacancy centers and multiparametric data analysis. *ACS Photonics* **6**, 1387–1392 (2019).
27. Berridge, M. J., Bootman, M. D. & Roderick, H. L. Calcium signalling: Dynamics, homeostasis and remodelling. *Nat. Rev. Mol. Cell Biol.* **4**, 517–529 (2003).
28. Block, B. A., O'Brien, J. & Meissner, G. Characterization of the sarcoplasmic reticulum proteins in the thermogenic muscles of fish. *J. Cell Biol.* **127**, 1275–1287 (1994).
29. Oyama, K. *et al.* Heat-hypersensitive mutants of ryanodine receptor type 1 revealed by microscopic heating. *Proc. Natl. Acad. Sci.* **119**(32), e2201286119 (2022).
30. de Meis, L. Brown adipose tissue Ca^{2+}-ATPase. *J. Biol. Chem.* **278**, 41856–41861 (2003).
31. Kondepudi, D. & Prigogine, I. *From Heat Engines to Dissipative Structures* (Wiley, 1998).
32. Guggenheim, E. *Modern Thermodynamics by the Methods of Willard Gibbs* (Methuen & Co Ltd., 1933).
33. Hamill, O. P., Marty, A., Neher, E., Sakmann, B. & Sigworth, F. J. Improved patch-clamp techniques for high-resolution current recording from cells and cell-free membrane patches. *Pflüg. Arch. Eur. J. Physiol.* **391**, 85–100 (1981).
34. Grynkiewicz, G., Poenie, M. & Tsien, R. Y. A new generation of Ca^{2+} indicators with greatly improved fluorescence properties. *J. Biol. Chem.* **260**, 3440–3450 (1985).
35. Steiner, P. *et al.* Modulation of receptor cycling by neuron-enriched endosomal protein of 21 kD. *J Cell Biol.* **157**(7), 1197–1209. https://doi.org/10.1083/jcb.200202022(2002).

Author contributions
Conceptualization: A.M.R., V.Z., E.G., A.R. and I.I.V.; methodology: A.M.R., V.Z., E.G., A.R. and I.I.V.; validation: A.M.R., V.Z.; formal analysis: A.M.R., V.Z., E.G.; investigation: A.M.R., V.Z., E.G.; resources: E.G., A.R. and A.G.S.; data curation: A.M.R.; writing—original draft: V.Z., A.M.R.; writing—review and editing: A.M.R., V.Z., E.G., A.R. and I.I.V.; supervision: A.R. and I.I.V.; project administration: I.I.V.; funding acquisition, V.Z., A.R. and A.G.S.

Competing interests
The authors declare no competing interests.

Additional information
Supplementary Information The online version contains supplementary material available at https://doi.org/10.1038/s41598-023-35141-4.

Correspondence and requests for materials should be addressed to A.M.R. or V.Z.

Reprints and permissions information is available at www.nature.com/reprints.

Publisher's note Springer Nature remains neutral with regard to jurisdictional claims in published maps and institutional affiliations.